

# Simultaneous joint inversion of MT and CSEM data using a multiplicative cost function

Aria Abubakar, Maokun Li, Jianguo Liu and Tarek M. Habashy, Schlumberger-Doll Research, Cambridge, MA, USA

## SUMMARY

We present an inversion algorithm to jointly invert controlled-source electromagnetic (CSEM) data and magnetotelluric (MT) data. CSEM and MT data provide complementary information about the subsea conductivity distribution, hence it is useful to derive earth conductivity models that simultaneously fit both data sets. One of the issues of this simultaneous joint inversion approach is how to assign the relative weight between CSEM and MT cost functions. In this work we propose a multiplicative cost function of the CSEM and MT data instead of the additive one. This multiplicative cost function mismatches does not require a choice of the relative weights between these two data sets. This cost function will adaptively put CSEM and MT data on equal footing in the inversion process. The inversion is accomplished with a regularized Gauss-Newton technique where the model parameters are forced to lie within their upper and lower bounds by a non-linear transformation procedure. A line search method is employed to enforce a reduction of the cost function at each iteration. We demonstrate the pros and cons of this joint inversion approach by using some synthetic examples.

## INTRODUCTION

The controlled-source electromagnetic (CSEM) technology has the potential of providing useful information in applications such as off-shore hydrocarbon exploration. With a horizontal electric dipole as a transmitter towed by a ship and multi-component electromagnetic receivers on the seafloor, this method has been applied in several field surveys. The high contrast in resistivity between saline-filled rocks and hydrocarbons (oil and gas), makes this method well-suited for detecting resistive targets (reservoirs), see Srnka (1986); Constable et al. (1986); Chave et al. (1991); MacGregor and Sinha (2000); Eidesmo et al. (2002). In order to make use of CSEM data one has to employed a non-linear inversion approach, for example see Abubakar et al. (2006); Commer and Newman (2006); ?)

The magnetotelluric (MT) method has a long history of use in diverse applications such as mining and geothermal explorations. It has also been applied in off-shore hydrocarbon explorations (for example, see Constable et al. (2008); Smirnov and Pedersen (2008)). MT data are largely insensitive to thin high resistivity targets that are associated with hydrocarbon deposits trapped in thin planar sedimentary layers. This is because MT, which uses naturally occurring signals as its sources, can be modeled as plane-waves. However, it is known that MT has a larger depth of investigation than CSEM. Hence, MT can be effectively used to obtain rough conductivity estimate of the subsurface. Similar to CSEM, interpretation of MT data has to be done using a full non-linear inversion approach, see Rodi and Mackie (2001); Kumar et al. (2007).

MT and CSEM data can provide complementary information: MT provides information of background conductivity structures, while CSEM identifies thin resistive targets. The same receivers can collect both CSEM and MT data, hence MT data come at a very low cost since they can be recovered from time series data when the transmitter is turned off. Usually CSEM and MT data are separately inverted. In the joint interpretation workflow, first MT data is inverted and then the results are used as an initial model for CSEM data inversion. Mackie et al. (2007) proposed a joint inversion method where one inverts both data sets simultaneously. By employing this approach they can obtain reasonable results with a reduced number of sources (for CSEM) and receivers. Commer and Newman (2008) also showed that one can significantly improve the inversion results by using this simultaneous joint inversion approach. However, both Mackie et al. (2007) and Commer and Newman (2008) point out that in this joint inversion approach one has to carefully choose the relative weighting between MT and CSEM data.

In this work we propose to use a multiplicative cost function for simultaneous joint inversion of MT and CSEM data. By using this cost function there is no need to choose the relative weighting between MT and CSEM data. This multiplicative cost function will effectively put equal weighting for both MT and CSEM data. This approach has also been employed before for multi-frequency electromagnetic inversions, see Abubakar and van den Berg (2000). Unlike Mackie et al. (2007) and Commer and Newman (2008), we employ the regularized Gauss-Newton approach as our inversion scheme. The general description of the forward algorithm can be found in Abubakar et al. (2008). The inversion algorithm is equipped with two different regularization functions to produce either a smooth (using a standard  $L_2$ -norm function) or a blocky (using a weighted  $L_2$ -norm function) conductivity distribution (van den Berg and Abubakar (2001)). To enhance the robustness of the algorithm, we incorporated a non-linear transformation for constraining the minimum and maximum values of the conductivity distribution (see Habashy and Abubakar (2004)). A line-search procedure for enforcing the error reduction in the cost function in the optimization process is also employed.

## INVERSION METHOD

We consider a non-linear inverse problem described by the following operator equations:

$$\mathbf{d}^C = \mathbf{s}^C(\mathbf{m}), \quad (1)$$

$$\mathbf{d}^M = \mathbf{s}^M(\mathbf{m}), \quad (2)$$

where

$$\mathbf{d}^C = [d^C(\mathbf{r}_i^S, \mathbf{r}_j^R, \omega_k), i = 1, 2, \dots, I; j = 1, 2, \dots, J; k = 1, 2, \dots, K]^T \quad (3)$$

## Simultaneous joint inversion of MT and CSEM data

is the vector of CSEM data and

$$\mathbf{d}^M = [d^M(\mathbf{r}_j^R, \omega_k), j = 1, 2, \dots, J; k = 1, 2, \dots, K^M]^T \quad (4)$$

is the vector of MT impedance data, in which  $\mathbf{r}_j^S$ ,  $\mathbf{r}_j^R$ , and  $\omega_k$  are the source positions, the receiver positions and the frequency of operation, respectively. The superscript  $T$  denotes the transpose of a vector. The vectors  $\mathbf{s}^C(\mathbf{m})$  and  $\mathbf{s}^M(\mathbf{m})$  represent simulated data computed by solving Maxwell equations. In CSEM the source is an electric dipole oriented parallel to the tow line and the receiver can be any component of the magnetic or electric field vector. In MT the source is a plane wave and the receivers measure the tangential components of both electric and magnetic fields. In this work we employed the two-and-half dimensional (2.5D) approximation for CSEM data, see Abubakar et al. (2008), and two-dimensional (2D) approximation for MT data.

The unknown vector of model parameters are defined as follows:

$$\mathbf{m} = [m(x_l, z_q), l = 1, \dots, L; q = 1, \dots, Q], \quad (5)$$

where  $x_l$  and  $z_q$  denote the center of the discretization cell. The unknown model parameter  $m(\mathbf{r}) = \sigma(\mathbf{r})/\sigma_0(\mathbf{r})$  is the normalized conductivity where  $\sigma_0(\mathbf{r})$  is the conductivity distribution of the initial model used in the inversion.

We pose the inverse problem as the minimization problem of a multiplicative cost function (Abubakar and van den Berg (2000); van den Berg and Abubakar (2001); Abubakar et al. (2008)) defined as follows:

$$\Phi_n(\mathbf{m}) = \phi^C(\mathbf{m}) \times \phi^M(\mathbf{m}) \times \phi_n^R(\mathbf{m}), \quad (6)$$

where

$$\phi^C(\mathbf{m}) = \frac{1}{2K^C} \sum_{k=1}^{K^C} \frac{\sum_{i=1}^I \sum_{j=1}^J |W_{i,j,k}^C [d_{i,j,k}^C - S_{i,j,k}^C(\mathbf{m})]|^2}{\sum_{i=1}^I \sum_{j=1}^J |W_{i,j,k}^C d_{i,j,k}^C|^2}, \quad (7)$$

$$\phi^M(\mathbf{m}) = \frac{1}{2K^M} \sum_{k=1}^{K^M} \frac{\sum_{j=1}^J |W_{j,k}^M [d_{j,k}^M - S_{j,k}^M(\mathbf{m})]|^2}{\sum_{j=1}^J |W_{j,k}^M d_{j,k}^M|^2}, \quad (8)$$

in which  $\mathcal{W}^C$  and  $\mathcal{W}^M$  are the data weighting matrices. The regularization cost function is given by

$$\phi_n^R(\mathbf{m}) = \sum_{\kappa=x,z} \int_D b_{\kappa,n}^2(x,y,z) \{ |\partial_{\kappa} \ln [m(x,z)]|^2 + \delta_n^2 \} dx dz, \quad (9)$$

in which  $\partial_x$  and  $\partial_z$  denote spatial differentiation with respect to  $x$  and  $z$  coordinate. The weights  $b_{\kappa,n}(x,z)$  are given by

$$b_{\kappa,n}^2(x,z) = \frac{1}{\int_D \{ |\partial_{\kappa} \ln [m_n(x,y,z)]|^2 + \delta_n^2 \} dx dz} \quad (10)$$

for the  $L_2$ -norm regularizer and

$$b_{\kappa,n}^2(x,z) = \frac{1}{V} \frac{1}{|\partial_{\kappa} \ln [m_n(x,z)]|^2 + \delta_n}, \quad V = \int_D dx dz \quad (11)$$

for the weighted  $L_2$ -norm regularizer as introduced in van den Berg and Abubakar (2001). The  $L_2$ -norm regularizer is known to favor smooth profiles, while the weighted  $L_2$ -norm regularizer is known for its ability to preserve edges. Note that for the  $L_2$ -norm regularizer, the weight  $b_{\kappa,n}(x,z)$  is independent of the spatial position. The positive parameter  $\delta_n$  is a constant that is chosen to be:

$$\delta_n^2 = \frac{\phi^C(\mathbf{m}_n) \phi^M(\mathbf{m}_n)}{\Delta x \Delta z}, \quad (12)$$

where  $\Delta x$  and  $\Delta z$  are discretization cell widths.

To solve equation (6) we employ a Gauss-Newton minimization approach. At the  $n^{\text{th}}$  iteration, we obtain a set of linear equations for the search vector  $\mathbf{p}_n$  that determines the minimum of the approximated quadratic cost function, namely,

$$\mathcal{H}_n \cdot \mathbf{p}_n = -\mathbf{g}_n. \quad (13)$$

where the gradient vector  $\mathbf{g}_n$  is given by

$$\begin{aligned} \mathbf{g}_n &= \phi^M(\mathbf{m}_n) \nabla \phi^C(\mathbf{m}) \Big|_{\mathbf{m}=\mathbf{m}_n} + \phi^C(\mathbf{m}_n) \nabla \phi^M(\mathbf{m}) \Big|_{\mathbf{m}=\mathbf{m}_n} \\ &\quad + \phi^C(\mathbf{m}_n) \phi^M(\mathbf{m}_n) \nabla \phi_n^R(\mathbf{m}) \Big|_{\mathbf{m}=\mathbf{m}_n}, \\ &= \phi^M(\mathbf{m}_n) \left\{ (\mathcal{J}_n^C)^T \cdot (\mathcal{W}^C)^T \cdot \mathcal{W}^C \cdot [\mathbf{d}^C - \mathbf{s}^C(\mathbf{m}_n)] \right\} \\ &\quad + \phi^C(\mathbf{m}_n) \left\{ (\mathcal{J}_n^M)^T \cdot (\mathcal{W}^M)^T \cdot \mathcal{W}^M \cdot [\mathbf{d}^M - \mathbf{s}^M(\mathbf{m}_n)] \right\} \\ &\quad + \phi^C(\mathbf{m}_n) \phi^M(\mathbf{m}_n) \mathcal{L}^{(1)}(\mathbf{m}_n) \cdot \mathbf{m}_n. \end{aligned} \quad (14)$$

The matrix  $\mathcal{J}_n^C$  and  $\mathcal{J}_n^M$  are the Jacobian matrices and

$$\left[ \mathcal{L}^{(1)}(\mathbf{m}_n) \cdot \mathbf{v} \right]_{l,q} = \frac{1}{m_{n;l,q}} \sum_{\kappa=x,z} \{ \partial_{\kappa} b_{\kappa,n} [\partial_{\kappa} \ln(v)] \}_{l,q}. \quad (15)$$

The Hessian matrix is given by

$$\begin{aligned} \mathcal{H}_n &= \phi^M(\mathbf{m}_n) \left[ (\mathcal{J}_n^C)^T \cdot (\mathcal{W}^C)^T \cdot \mathcal{W}^C \cdot \mathcal{J}_n^C \right] \\ &\quad + \phi^C(\mathbf{m}_n) \left[ (\mathcal{J}_n^M)^T \cdot (\mathcal{W}^M)^T \cdot \mathcal{W}^M \cdot \mathcal{J}_n^M \right] \\ &\quad + \phi^C(\mathbf{m}_n) \phi^M(\mathbf{m}_n) \mathcal{L}^{(2)}(\mathbf{m}_n). \end{aligned} \quad (16)$$

In order to make the Hessian matrix non-negative definite, we neglect the second order derivatives of the cost function  $\phi^C(\mathbf{m})$  and  $\phi^M(\mathbf{m})$ , and the non-symmetric terms. The Hessian of the regularization cost function is given by

$$\left[ \mathcal{L}^{(2)}(\mathbf{m}_n) \cdot \mathbf{v} \right]_{l,q} = \frac{1}{m_{n;l,q}} \sum_{\kappa=x,z} \left\{ \partial_{\kappa} b_{\kappa,n} \left[ \partial_{\kappa} \left( \frac{v}{m_n} \right) \right] \right\}_{l,q}, \quad (17)$$

where we have neglected the non-symmetric term. Note that in equations (14) and (16) we used the fact that  $\phi_n^m(\mathbf{m}_n) = 1$ . Note also that for this multiplicative cost function the gradient is exact, however the Hessian matrix is an approximate one since we neglected the 2nd order derivative and the non-symmetric terms.

After the Gauss-Newton search vector  $\mathbf{p}_n$  is obtained by solving the linear system of equations in equation (13) using a conjugate gradient least-square (CGLS) technique (see Golub and

## Simultaneous joint inversion of MT and CSEM data

Van Loan (1996)), the unknown model parameters are updated using a non-linear transformation and the line-search procedure described in Habashy and Abubakar (2004).

This multiplicative cost function in equation (6) will put both MT and CSEM cost function equally important. This is achieved by using the MT data cost function at previous iteration  $\phi^M(\mathbf{m}_n)$  as the weight for the CSEM cost function and vice versa, see equations (14) and (16).

As for the weight for the regularization factor, a large weight at the beginning of the optimization process is used because the values of  $\phi^C(\mathbf{m})$  and  $\phi^M(\mathbf{m})$  are still large. In this case, the search direction is predominantly a steepest descent, which is more appropriate to use in the initial steps of the iteration process because it has a tendency to suppress large swings in the search direction. As the iteration proceeds, the optimization process will gradually reduce the error in the data misfit while the regularization factor  $\phi_n^R(\mathbf{m})$  remains at a nearly constant value close to unity. In this case, the search direction corresponds to a Newton search direction, which is more appropriate to use as we get closer to the minimum of the data misfit cost function of either  $\phi^C(\mathbf{m})$  or  $\phi^M(\mathbf{m})$  where the quadratic model of the cost function becomes more accurate. If noise is present in the data, the data misfit cost functions  $\phi^C(\mathbf{m})$  and  $\phi^M(\mathbf{m})$  will plateau to certain values determined by the signal-to-noise ratio; hence, the weight, on the regularization factor will be non-zero. In this way, the noise will, at all times, be suppressed in the inversion process and the need for a larger regularization when the data contains noise will be automatically fulfilled.

### NUMERICAL EXAMPLE

To illustrate the method we present a synthetic data inversion example, in which a single thin reservoir is embedded in a non-flat layered formation. The conductivity distribution of this model is shown in Figure 1(a) and the colorbar are in a reverse log-scale. The seabed consists of three non-flat layers. Their conductivities (from top to bottom) are 0.6, 0.3 and 0.15 S/m. A reservoir of 8 km wide and 150 m thick is located in the middle seabed layer. Its conductivity is 0.02 S/m. The sea-water depth is 1 km and the water conductivity is 3 S/m.

In the survey, we employed twenty-one receivers located at the sea-floor. The receivers are deployed uniformly from -10 km to 10 km. They record both CSEM and MT data and they are indicated by circles in Figure 1. For CSEM data we invert only the in-line fields (horizontal fields in the tow direction) while for MT data we employed both TE and TM polarization impedances. The CSEM transmitter is assumed to be towed from -10 to 10 km at 50 m above the receivers. In the inversion we use CSEM data every 500 m. We employed two CSEM frequencies (0.25 and 0.75 Hz) and eight MT frequencies (0.005, 0.01, 0.025, 0.05, 0.1, 0.25, 0.5 and 1 Hz). We also added two-percent white noise to the synthetic data.

In the inversion we employed a domain of 36 km by 6 km with grid size 200 m by 75 m. The number of unknowns is 14,400. As the initial model we use a model with homogeneous seabed

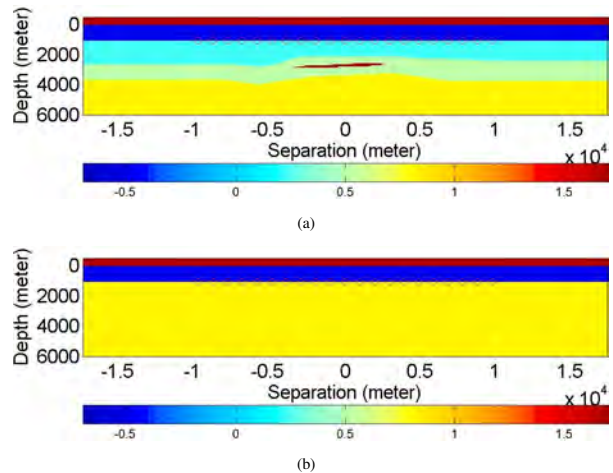


Figure 1: A single-reservoir model embedded in a layered seabed: (a): True model; (b): Initial model.

as shown in Figure 1(b). The homogeneous seabed conductivity is 0.15 S/m.

Figure 2(a) shows the reconstructed image using only MT data. We observe that the three seabed layers are properly reconstructed both in shape and conductivity values, however we failed to detect the presence of the reservoir. This reflects the limitation of the physics of MT data where the low-frequency electromagnetic plane waves can have a large depth of investigation and good horizontal resolution, however they lack good vertical resolution. Note that regions  $x < -10$  km and  $x > 10$  km are not well-reconstructed because we do not have sources and receivers in these regions. The inversion results of CSEM data are given in Figure 2(b). In this case we manage to obtain a rough estimate of the reservoir, however the layered formation is not properly reconstructed. This is mainly because of the limited depth of investigation of CSEM data.

Figure 2(c) shows the joint inversion result using both CSEM and MT data. We observe that the reservoir and the layers are now both well reconstructed. The MT data are sensitive to the layering structures and CSEM data are sensitive to the thin resistive layer. From the results, we observe that the CSEM and MT joint data inversion can provide improved inversion result. We present also the normalized data misfits (these are the value of the CSEM and MT cost functions without  $\mathcal{W}^C$  and  $\mathcal{W}^M$ ) in Figure 3 for every data frequency at each Gauss-Newton iteration of the joint CSEM and MT data inversion run.

### CONCLUSION

We presented an inversion algorithm to jointly invert controlled-source electromagnetic (CSEM) data and magnetotelluric (MT) data. One of the issues of this simultaneous joint inversion approach is how to assign the relative weights between CSEM and MT data. In this work we proposed to minimize the product of CSEM and MT cost functions instead of the traditional

## Simultaneous joint inversion of MT and CSEM data

additive one. In this multiplicative cost function there is no need to choose the relative weighting between these two data sets. This cost function will effectively put CSEM and MT data on equal footing in the inversion process. The effectiveness of this approach was demonstrated using a synthetic example.

### ACKNOWLEDGMENTS

We thank Dr. V. Druskin of Schlumberger-Doll Research, Cambridge, MA, USA and Dr. L. Knizhnerman of the Center for Geophysical Expedition, Moscow, Russia for providing the 2.5D finite-difference forward program.

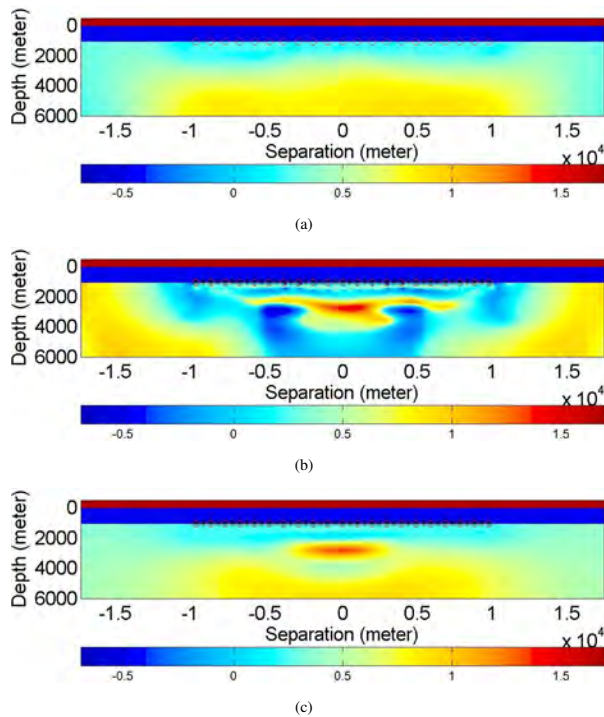


Figure 2: Inversion of a single-reservoir model embedded in layered seabed: (a): Inverted model using only MT data; (b): Inverted model using only CSEM data; (c): Inverted model using both CSEM and MT data inverted jointly.

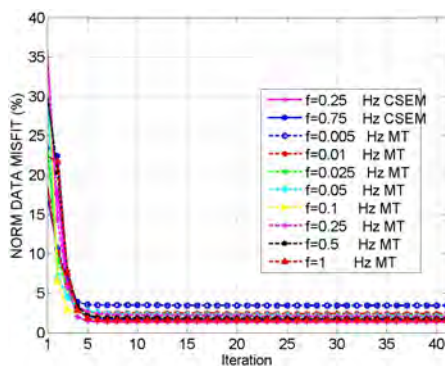


Figure 3: Plot of data misfit in every iteration of joint CSEM and MT data inversion.

## EDITED REFERENCES

Note: This reference list is a copy-edited version of the reference list submitted by the author. Reference lists for the 2009 SEG Technical Program Expanded Abstracts have been copy edited so that references provided with the online metadata for each paper will achieve a high degree of linking to cited sources that appear on the Web.

## REFERENCES

- Abubakar, A., T. Habashy, V. Druskin, D. Alumbaugh, A. Zerelli, and L. Knizhnerman, 2006, Two-and-half dimensional forward and inverse modeling for marine CSEM problems: 76th Annual International Meeting, SEG, Expanded Abstracts, 750–754.
- Abubakar, A., T. Habashy, V. Druskin, L. Knizhnerman, and D. Alumbaugh, 2008, 2.5D forward and inverse modeling for interpreting low-frequency electromagnetic measurements: *Geophysics*, **73**, no. 4, F165–F177.
- Abubakar, A., and P. van den Berg, 2000, Iterative reconstructions of electrical conductivity from multiexperiment low-frequency electromagnetic data: *Radio Science*, **35**, 1293–1306.
- Chave, A. D., S. C. Constable, and R. N. Edwards, 1991, Electrical exploration methods for the seafloor, in M. N. Nabighian, ed., *Electromagnetic methods in applied geophysics*: SEG, **2**, 931–966.
- Commer, M., and G. A. Newman, 2006, Large scale 3D EM inversion using optimized simulation grids non-conformal to the model space: 76th Annual International Meeting, SEG, Expanded Abstracts, 760–764.
- , 2008, Optimal conductivity reconstruction using three-dimensional joint and model-based inversion for controlled-source and magnetotelluric data: 78th Annual International Meeting, SEG, Expanded Abstracts, 609–613.
- Constable, S. C., C. S. Cox, and A. D. Chave, 1986, Offshore electromagnetic surveying techniques: 66th Annual International Meeting, SEG, Expanded Abstracts, 81–82.
- Constable, S., K. Key, and L. Lewis, 2008, Mapping offshore sedimentary structure using electromagnetic methods and terrain effects in marine magnetotelluric data: *Geophysical Journal International*, **176**, 431–442.
- Eidesmo, T., S. Ellingsrud, L. M. MacGregor, S. Constable, M. C. Sinha, S. Johansen, F. N. Kong, and H. Westerdahl, 2002, Sea bed logging (SBL), a new method for remote and direct identification of hydrocarbon filled layers in deepwater areas: *First Break*, **20**, 144–152.
- Golub, G. H., and C. F. Van Loan, 1996, *Matrix computations*, 3rd ed.: Johns Hopkins Univ. Press.
- Habashy, T. M., and A. Abubakar, 2004, A general framework for constraint minimization for the inversion of electromagnetic measurements: *Progress In Electromagnetics Research*, **46**, 265–312.
- Kumar, A., L. Wan, and M. S. Zhdanov, 2007, Regularization analysis of three-dimensional magnetotelluric inversion: 77th Annual International Meeting, SEG, Expanded Abstracts, 482–486.
- MacGregor, L., and M. Sinha, 2000, Use of marine controlled source electromagnetic sounding for sub-basalt exploration: *Geophysical Prospecting*, **48**, 1091–1106.
- Mackie, R., M. D. Watts, and W. Rodi, 2007, Joint 3D inversion of marine CSEM and MT data: 77th Annual International Meeting, SEG, Expanded Abstracts, 574–578.
- Rodi, W., and R. Mackie, 2001, Nonlinear conjugate gradients algorithm for 2-D magnetotelluric inversion: *Geophysics*, **66**, 174–187.
- Smirnov, M. Y., and L. B. Pedersen, 2008, Magnetotelluric measurements across the Sorgenfrei-Tornquist Zone in southern Sweden and Denmark: *Geophysical Journal International*, **176**, 443–456.
- Srnka, L. J., 1986, Methods and apparatus for offshore electromagnetic sounding utilizing wavelength effects to determine optimum source and detector positions: U. S. Patent 4,617,518.
- van den Berg, P. M., and A. Abubakar, 2001, Contrast source inversion method: State of art: *Progress In Electromagnetic Research*, **34**, 189–218.